

Provided for non-commercial research and education use.
Not for reproduction, distribution or commercial use.



This article appeared in a journal published by Elsevier. The attached copy is furnished to the author for internal non-commercial research and education use, including for instruction at the authors institution and sharing with colleagues.

Other uses, including reproduction and distribution, or selling or licensing copies, or posting to personal, institutional or third party websites are prohibited.

In most cases authors are permitted to post their version of the article (e.g. in Word or Tex form) to their personal website or institutional repository. Authors requiring further information regarding Elsevier's archiving and manuscript policies are encouraged to visit:

<http://www.elsevier.com/copyright>



ELSEVIER

available at www.sciencedirect.comjournal homepage: www.elsevier.com/locate/agwat

Prediction of the soil-depth salinity-trend in a vineyard after sustained irrigation with saline water

W.P. de Clercq ^{a,*}, M. Van Meirvenne ^b, M.V. Fey ^a

^a Soil Science, Stellenbosch University, Private Bag X1, Matieland 7602, South Africa

^b Soil Management and Soil Care, Ghent University, Ghent, Belgium

ARTICLE INFO

Article history:

Received 27 February 2008

Accepted 4 September 2008

Published on line 16 October 2008

Keywords:

Grapevines

Soil salinity profiles

Suction cup lysimetry

Salt accumulation

Sustainable irrigation

Trend surface analysis

ABSTRACT

Remote sensing combined with an ability to look deeper than the soil surface is currently high in demand. This study was conducted through scaling down the amount of soil data from a saline irrigation water experiment to see if one can still capture the essential soil salinity depth trends within the data, to a level that can enhance the ability of remote methods. A saline irrigation experiment with 6 water qualities was conducted for 8 years on 1.2 ha of vineyard land near Robertson in the Western Cape Province of South Africa. Soil water was sampled at regular intervals at 5 depths between 0.15 and 1.2 m with suction cup lysimeters at a fixed time following each irrigation. Electrical conductivity of the soil water (EC_{sw}) was determined after sampling. Data collected over the full 8-year period were investigated for depth trends in EC_{sw} , seeking trend lines with lowest polynomial order that were still significantly predict the salinity profile. At all treatment levels a first order polynomial equation, fitted to the salinity profiles, significantly predicted the salinity trends. The EC_{sw} value at only two depths could therefore be used to calculate total salt accumulation and soil water quality below the root zone. The implication is that considerable value can be obtained from minimal measurements both in estimating salt accumulation in the soil profile and predicting water quality in return flow from saline irrigation.

© 2008 Elsevier B.V. All rights reserved.

1. Introduction

There are scant reports on soil water salinity dynamics in response to saline irrigation, especially concerning the seasonal variation in electrical conductivity of the soil water (EC_{sw}) as a function of depth. Among others, Rhoades et al. (1997), Cetin and Kirda (2003), De Clercq and Van Meirvenne (2005) and Douaik et al. (2006) have all emphasised the importance of spatial and temporal changes in soil salinity and the effect on return-flow water-quality when use is made of low quality irrigation water. In such studies, soil salinity is generally reported as an integrated value for the whole profile.

In many countries sustained irrigation with poor quality water is commonly practised and requires close monitoring and control of soil salinity at both regional and field scales to minimise the adverse effects on production and impacts on downstream users (Odeh et al., 1998; Kelleners and Chaudhry, 1998; Kotb et al., 2000; Görgens and De Clercq, 2006). Rapid assessment of soil salinity is becoming increasingly important for managerial purposes. Salinity depth trends were investigated after sustained irrigation for sugar cane (Nelson and Ham, 2000), winter wheat (Sharma and Rao, 1998) and rice (Mondala et al., 2001). For vineyards, De Clercq et al. (2001) reported on the effects of poor quality irrigation and posed the

* Corresponding author.

E-mail address: wpdc@sun.ac.za (W.P. de Clercq).

following list of questions that should be considered when considering irrigation quality:

1. Does the farmer use refined scheduling techniques?
2. Do the advantages of partial wetting of the soil apply?
3. What is the salt tolerance of the crop?
4. Does the salt content of the marketable product matter?
5. What is the length of season for the crop?
6. What is the typical rooting volume of the crop?
7. Under saline conditions, should crops be selected with the smallest possible rooting volume?
8. What is the quality of the receiving waters?

A number of articles found, where the electrical conductivity measured alone or where for instance time domain reflectometry was used refer to soil water content and bulk electrical conductivity, indicated a very complicated approach to link soil water electrical conductivity (EC) with other measured parameters. [Persson and Bertacchi Uvo \(2003\)](#) is perhaps the most recent example of the complicated situation arising when soil water EC is measured at a range of soil water content values for different soils. These are all at non-saturated conditions. The ability to use these values for any predictions depends on the accuracy of two infield-measured parameters and the calibration of the individual sensors. These measurements can be of great value when plant reaction to soil water EC needs to be tested between irrigations but to compare results between different locations and different instruments becomes quite a daunting task. [De Clercq et al. \(2001\)](#) showed that the cumulative effect of bad irrigation water quality on vines could be adequately described using a single set of soil water measurements taken after each irrigation event, when the soil water content was still at field water capacity. These soil water samples, extracted from the soil using micro lysimetry, were then analysed using a single laboratory EC probe. This method then allowed for easier comparison between infield measurements done at different depths and locations and different soil types. Using the extracted soil water at field capacity also has the added advantage that it can be directly related to the quality of the water that moved through the soil. Once evaporation from the soil surface starts and the plant starts to utilise some of the water, the downward movement of water stops and the EC_{sw} starts to change, as salts are concentrated in the remaining soil water.

Modern devices, such as the electromagnetic induction sensor EM38, used for routine monitoring of soil salinity, are limited in its ability to make measurements over the entire soil profile. [Shi et al. \(2006\)](#) indicated that they could successfully map coastal sandy soils for reclamation using hyperspectral remote sensing; however, their study applied only to soil surface conditions. On the other hand, [Zhu et al. \(2007\)](#)

developed a knowledge based system for predicting grain yield taking into account all possible conditions affecting wheat growth, including soil type and soil-depth parameters. If these two approaches could be combined, the possibility of predicting subsoil conditions remotely seems attainable. [Farifteh and Farshad \(2002\)](#) emphasized the need to be able to detect and model soil properties from remotely sensed sources. They listed some possibilities of how to be able to tell more about subsoil conditions, in particular soil salinity, from remotely sensed information. They indicated that imaging spectrometry provides large volumes of high resolution spectral data, which can be useful to detect soil properties. They further indicated that a next step would be to link modelled soil processes using existing models (for example SWAP and CropSyst) to this hyperspectral information base, to model subsoil conditions and the fate of salinity in the landscape.

[Metternicht and Zinck \(2003\)](#) indicated in a review article some constraints on the use of remote sensing data. They stated that monitoring soil salinity cannot be achieved from remote sensing data alone and requires a solid synergy between remote sensing data, field observations and laboratory determinations as sources of data, and GIS capabilities for processing, transforming and displaying the data. They further concluded that the best results are obtained when integrating remote sensing data with field and laboratory data and that it is the researcher's challenge to identify the most adequate salinity indicators for a particular area, so that appropriate ground and remote sensing techniques can be applied to extract information in an accurate and cost-effective manner. [Lesch et al. \(1995\)](#) attempted the link between satellite imagery and EM38 interpreted soil salinity information using multiple linear regression models and found, after successful modelling, that they could reduce the sampling density and still retain the prediction accuracy inherent in their statistical calibration techniques, also facilitating assessment methodology that can be applied in a rapid, practical, and cost-effective manner.

This article strives to find means of revealing more about irrigated subsoil conditions when using remotely sensed information. For that purpose, it is important to find and define subsoil conditions that lend itself to a higher degree of predictability and define a starting point for modelling of this nature. Therefore, a basis needs to be established for making the best use of relatively meagre information about the salinity depth function. To achieve this goal we used the approach posed by [Davis \(1986\)](#) to use a F-test ([Tables 1 and 2](#)) coupled with trend surface theory ([Davis, 1986, pp. 405–422](#)) to find trend lines with the highest significance and with the lowest possible polynomial order. The procedure aims to solve curvilinear regressions or trend surfaces in the simplest possible way and the idea was developed before computers

Table 1 – ANOVA table for a linear surface trend (n = number of observations)

Variance	Sum of squares	d.f.	Mean SS	F-test
Linear trend	SS _r	2	MS _r	$F = MS_r/MS_a$
Deviation	SS _a	$n - 2 - 1$	MS _a	
Total variance	SS _t	$n - 1$		

Table 2 – ANOVA table for the significance of increase in order from p to $p + 1$ where the trend surface of order p has k regression coefficients (without b_0) and surface of order $p + 1$ have m regression coefficients (without b_0)

Variance object	Sum of squares	d.f.	Mean SS	F-test
Trend surface order $p + 1$	SS_{T_p+1}	m	MS_{T_p+1}	$F_{p+1} = MS_{T_p+1}/MS_{A_{p+1}}^a$
Deviation from order $p + 1$	$SS_{A_{p+1}}$	$n - m - 1$	$MS_{A_{p+1}}$	
Trend surface of order p	SS_{T_p}	k	MS_{T_p}	$F_p = MS_{T_p}/MS_{A_p}^b$
Deviation from order p	SS_{A_p}	$n - k - 1$	MS_{A_p}	
Increase in order	$SS_V = SS_{T_p+1} - SS_{T_p}$	$m - k$	MS_V	$F_V = MS_V/MS_{A_{p+1}}^c$
Total variance	SST	$n - 1$		

The number of observations is n .

^a Significance test for trend surface with order $p + 1$.

^b Significance test for trend surface with order p .

^c Significance test for the increase in order.

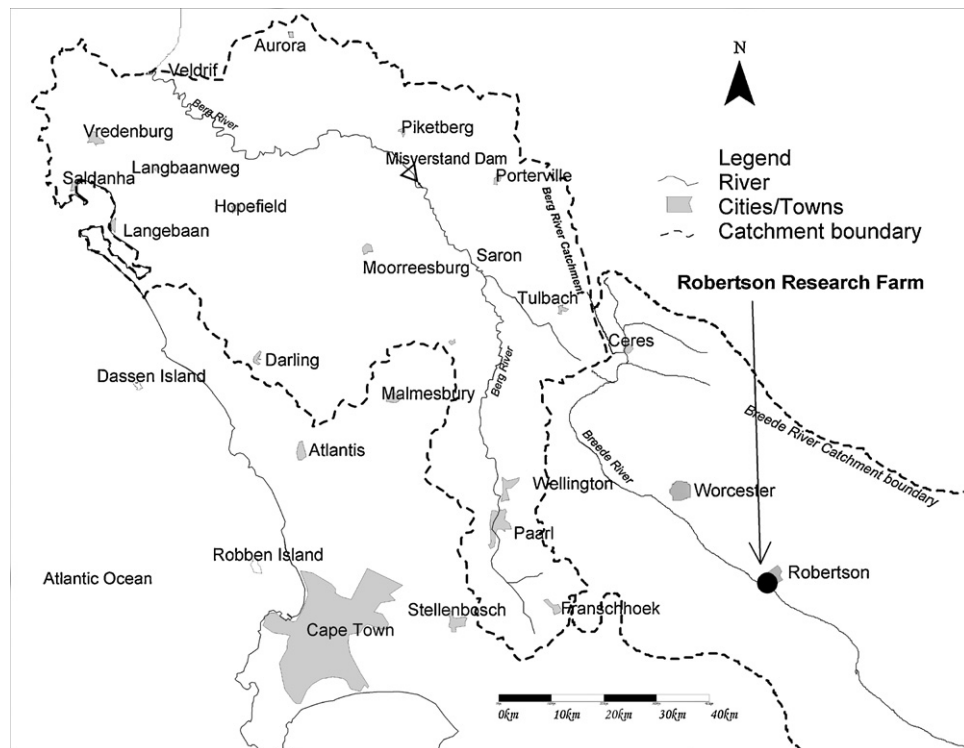
became widely available. The choice of a polynomial expression is normally governed by the goal of achieving the highest degree of goodness-of-fit and higher order polynomials are more successful at this since they encompass the lower order forms (Mondala et al., 2001). However, higher order polynomials require more parameters to be fit and therefore they are more data demanding. Frequently by making use of an adjusted R^2 -value, deviation from the trend surface and the degrees of freedom, the decision for using a lower order polynomial also becomes evident. Therefore, for small data sets, lower order polynomials are usually more realistic (Lesch et al., 1995).

We know that the knowledge base for modelling soil salinity is well established and similarly the methodology for mapping features of the topsoil from remote sources. The linkup between the two, that could allow us to know more about the soil from the interpretation of remotely sensed information, is currently

fuzzy. The objective of this paper therefore is to examine soil-depth salinity-trends after prolonged irrigation of a vineyard with different salt concentrations, and to find the simplest basis for calculating salt accumulation and return flow water quality from a limited number of measurements that could also be detected remotely.

2. Materials and methods

A saline irrigation experiment was carried out for 8 years (from 1991 till 1998) in a vineyard near Robertson in the Western Cape Province, South Africa (Fig. 1, central coordinates $33^{\circ}49'29.03''S$; and $19^{\circ}52'44.77''E$). The vineyard was established in 1974 with Colombar vines, grafted on Richter-99 rootstock and trained on a factory roof trellising system (Saayman, 1988). Van Zyl (1984) described the soil as a Hutton

**Fig. 1 – Map of a section of the Western Cape region of South Africa, indicating the location of the Robertson research farm.**

fine sandy loam. In terms of the current South African soil classification (Soil classification working group, 1991) the soil belongs to the Trawal 2210 family (Typic Durochrepts according to USDA Soil Taxonomy), with an ortic A-horizon of about 0.15 m depth and a neo-carbonate B-horizon down to a duripan at about 1.2 m depth. Soil preparation included homogenising by deep cultivation to about 1 m prior to planting.

2.1. The experimental layout

The 1.2 ha experimental block was divided into 24 plots to which were randomly allocated 4 replications of 6 irrigation salinity treatments. The six treatments were $\sim 0.23, 0.75, 1.5, 2.5, 3.5$ and 5.0 dS m^{-1} , the first being normal canal water and the others canal water to which CaCl_2 and NaCl had been added in a 1:1 molar ratio to achieve the desired salinity. Irrigation was applied with micro jet sprinklers. Only two thirds of the total soil surface was wetted by irrigation, i.e., each vine had a soil surface of 3 m^2 and therefore only 2 m^2 was wetted. Scheduling was done according to water use of the least saline plots, being those that received canal water and the soil water deficits were calculated from weekly neutron probe measurements. Irrigation applications included a 10 percent leaching fraction which is standard practice in the region. The experimentally determined mean field capacity of $287 \text{ mm } 1.05 \text{ m}^{-1}$, which is equivalent to 273 mm m^{-1} , was used to determine the soil water deficit in the control plots. This was described in full by De Clercq et al. (2001).

This is a predominantly winter rainfall region, which ensured that there was negligible interference in the water balance by rainfall during the summer months when most of the irrigation was applied. The average total amount of irrigation applied during summer was 600 mm and the combined winter rainfall and winter irrigation was aimed at 600 mm. During winter, rain was supplemented with irrigation to promote leaching of salts and ensure the success of a cover crop (De Clercq et al., 2001).

Each plot consisted of five vine rows, 3 m apart, with 23 vines per row at 1 m spacing. The roots of the vines typically lie between 10 and 80 cm depth with the bulk of the roots between 30 and 60 cm depth. Soil measurements were confined to the central ten vines in the middle row of each plot. Suction cup lysimeters (SCL) were installed between two of these vines at depths of 15, 30, 60, 90 and 120 cm and linked to a central vacuum pump. The vacuum pump was synchronised with an irrigation controller allowing remote control of soil water extraction. All of the 120 soil water samples were thus taken simultaneously at exactly the same time after each irrigation event. After collection of the soil water samples, the EC was measured for each, using a normal laboratory EC meter under normal laboratory conditions (De Clercq et al., 2001).

Irrigation was systematically applied in the afternoon of each Wednesday and suction sampling was initiated 12 h after irrigation had terminated, to ensure that the soil water status was effectively at field capacity. Over the 8-year duration of the experiment at least 12 annual sets of suction cup data were successfully collected, with 7–9 of these being collected during the irrigation season and the remainder during winter (De Clercq et al., 2001).

2.2. Data analysis

Trend surface analysis, as described by Davis (1986), was used to analyse the seasonal soil salinity distribution with depth. In this procedure the order of the polynomial expressions, fitted to the EC_{sw} data (Z) plotted as a function of time (X) and depth (Y) for each treatment, was raised successively to establish the polynomial with the lowest order that was still significant.

To simplify the trend surface routine, an algorithm was developed in Basic programming language, which determines the coefficients (b_0, b_1, b_2) relating X, Y and Z to each other for n observations in the following three equations:

$$\sum Z = b_0 n + b_1 \sum X + \sum Y \quad (1)$$

$$\sum XZ = b_0 \sum X + b_1 \sum X^2 + b_2 \sum XY \quad (2)$$

$$\sum YZ = b_0 \sum Y + b_1 \sum XY + b_2 \sum Y^2 \quad (3)$$

Having derived these coefficients, the position of Z on a linear surface trend (i.e. EC_{sw} as a function of depth and time) can be predicted. The goodness of fit of this surface trend can be calculated from the total sum of squares (SS_t) and the sums of squares resulting from the trend surface (SS_r), and the deviation from the trend surface (SS_a), where

$$\text{SS}_a = \text{SS}_t - \text{SS}_r \quad (4)$$

and the goodness of fit is then calculated as

$$R^2 = \frac{\text{SS}_r}{\text{SS}_t} \quad (5)$$

with R^2 being a multiple synonym for the R^2 used in linear regression. Using Eq. (4) in (5), R^2 can be rewritten as:

$$R^2 = \frac{\text{SS}_r}{\text{SS}_t} = 1 - \frac{\text{SS}_a}{\text{SS}_t} \quad (6)$$

Because R^2 is enhanced by increasing the order of the polynomial describing the trend surface, it has doubtful value for decision making. We therefore adopted an adjusted R^{2*} which is calculated in terms of SS_a in (6) and not SS_r in (5), and then corrected for degrees of freedom (d.f.),

$$\begin{aligned} R^{2*} &= 1 - \left(\frac{\text{SS}_a}{n - k - 1} \right) \cdot \left(\frac{\text{SS}_t}{n - 1} \right)^{-1} \\ &= 1 - (1 - R^2) \cdot \left(\frac{n - 1}{n - k - 1} \right) \end{aligned} \quad (7)$$

where the numerator terms $n - 1$ and $n - k - 1$ are the d.f., in which n is the number of observations and k is the number of regression coefficients ignoring b_0 .

The most important argument for using trend surface analysis in the current context lies in the test for significance (F-test, Tables 1 and 2). The significance of the specific trend was tested through an analysis of variance or ANOVA (Table 1). The degrees of freedom used (d.f. minus b_0) were 2 for the 1st order polynomial, 5 for the 2nd order and 9 for the 3rd order. The test for significance was then applied and compared for surface trends of different order in an expanded ANOVA

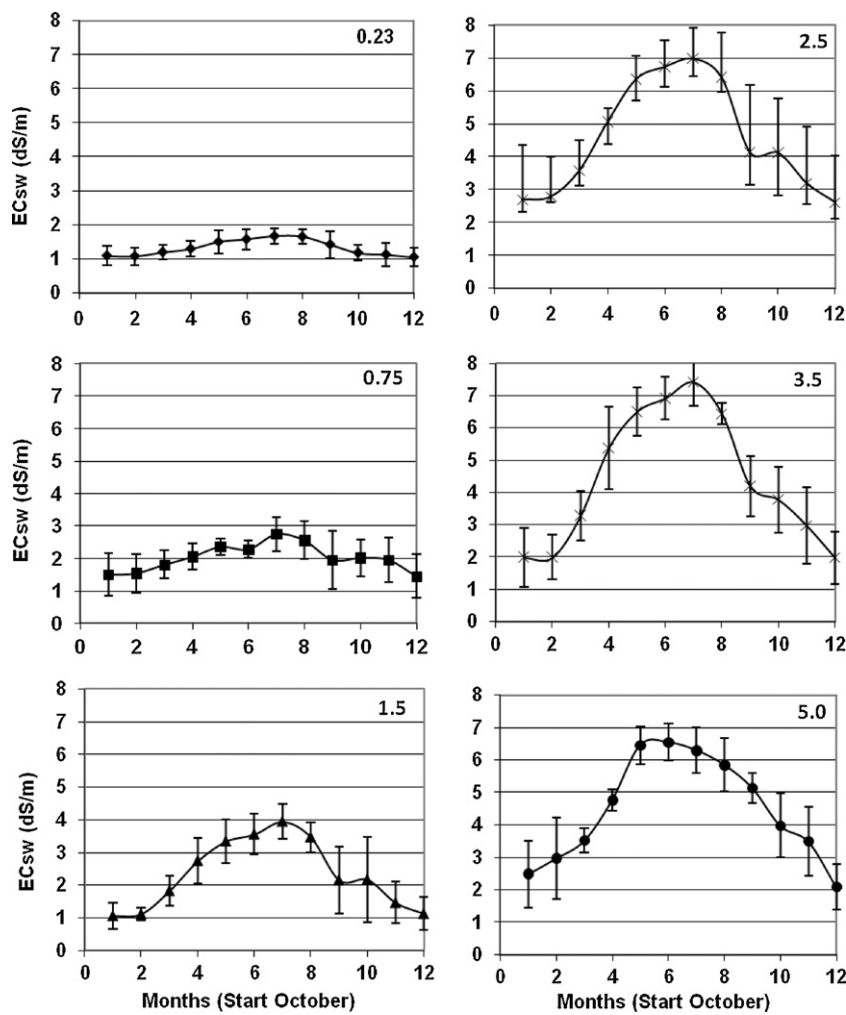


Fig. 2 – Monthly means and standard deviations (vertical bars), calculated for an 8-year period, of soil water salinity developed in response to six irrigation salinity treatments (dS m^{-1}).

(Table 2). For each increase in order the significance of the increase was also tested. The expanded ANOVA in Table 2 consisted of three variance analyses, each with its own F-value.

This resulted in two estimates for Z: one from a trend surface of order p and one from a trend surface of order $p + 1$. For each of these estimates, two sums of squares were calculated for the fitted trend surface (SS_{Tr_p} and $\text{SS}_{\text{Tr}_{p+1}}$) and two for the deviation from the fitted trend (SS_{A_p} and $\text{SS}_{\text{A}_{p+1}}$). The

latter were derived from SS_{Tr} , and SS_{Tr_p} or $\text{SS}_{\text{Tr}_{p+1}}$, respectively. The sum of squares that originates through the increase in order is $\text{SS}_v = \text{SS}_{\text{Tr}_{p+1}} - \text{SS}_{\text{Tr}_p}$. Dividing these sums of squares by their respective d.f., produces R^2 * (adjusted R^2) values which can then be compared by means of the three F-tests.

The above approach formed the basis for deciding which order of trend surface to use for predicting EC_{sw} as a function of soil depth and time of year. Through this collective approach, an argument can be substantiated that whatever

Table 3 – Summer month (October–March) statistics for EC_{sw} (dS m^{-1}) as a function of irrigation salinity treatments ($n = 192$ observations per treatment)

Treatment (dS m^{-1})	0.23	0.75	1.5	2.5	3.5	5.0
Min	0.75	0.80	0.67	1.26	1.12	1.14
Max	2.07	2.61	4.53	7.54	7.58	6.90
Mean	1.28	1.92	2.27	4.55	4.34	4.31
s^2	0.06	0.10	0.21	0.35	0.40	0.29
Skewness	0.52	-0.78	0.30	-0.17	0.06	-0.30
Kurtosis	0.69	-0.45	-1.10	-1.19	-1.47	-0.89

s^2 is an estimator of the variance σ^2 .

Table 4 – ANOVA table for a linear surface trend (cf. Table 1)

Variance object	Sum of squares (SS)	d.f.	Mean SS	F-test
Trend surface order p	29088	2	13158	128
Deviation from surface	26316	27	102	
Total variance	2772	29		$F(0.05, 2, 27) = 2.62$

Table 5 – ANOVA table for the significance of an increase in order p to $p + 1$ where the trend surface with order p has k regression coefficients (without b_0) and the trend surface with order $p + 1$ has m regression coefficients (without b_0)

Variance object	Sum of squares (SS)	d.f.	Mean SS	F-test
Trend surface, order $p + 1$	26702	5	5340	53.7 ^a
Deviation from surface	2386	24	99	$F(0.05, 5, 24) = 2.62$
Trend surface, order p	26316	2	13158	128.13 ^b
Deviation from surface	2772	27	102	$F(0.05, 2, 27) = 3.36$
Increase in order	386	3	128	1.294 ^c
Total variance	29088	29		$F(0.05, 3, 24) = 3.01$

The number of observations is n (cf. Table 2).

^a Significance test of trend surface with order $p + 1$.

^b Significance test of trend surface with order p .

^c Significance test of the increase in order.

polynomial trend applies for a trend surface, should apply for an individual soil profile.

3. Results and discussion

All EC_{sw} data collected in each month over 8 irrigation years were pooled to allow monthly means and standard deviations to be calculated over all depths for each treatment. These were plotted from October onwards for the six salinity treatments and shown in Fig. 2. It can be observed that the salinity peak between March and May increased in magnitude over the first four levels of irrigation salinity but remained relatively constant thereafter, suggesting that there is a characteristic upper limit of profile salinity governed by the application of a 10 percent leaching fraction in combination with leaching by winter rain. This also suggests that in the high salinity treatments the water uptake was reduced and that as a result

the leaching fraction may have been larger than the planned 10 percent. A number of studies showed the effects of salinity on crop yield, by relating the effect soil salinity has on crop ET, and assuming the ET and crop yield to be linearly related (Shani et al., 2007; Ben-Gal et al., 2008).

The summer data (October–March) for each treatment (192 measurements per treatment) were pooled for the purpose of calculating the statistics shown in Table 3. These summer data formed the basis for developing predictive polynomial expressions relating soil salinity to both depth and time. The procedure of Davis (1986) was applied to identify the polynomial with the lowest order while remaining statistically significant in 95% of the cases. The significance of the increase in trend surface order was tested and the results are shown in Tables 4–6. These tables show the significance, in terms of F values, of first, second and third order polynomials. The $F(p, d.f., d.f.)$ value is also shown in each case and the latter is consistently smaller than the F value, supporting the argu-

Table 6 – ANOVA table for the significance of an increase in order from $p + 1$ to $p + 2$ where the trend surface with order $p + 1$ has k regression coefficients (without b_0) and the trend surface with order $p + 2$ has m regression coefficients (without b_0)

Variance object	Sum of squares (SS)	d.f.	Mean SS	F-test
Trend surface, order $p + 2$	27793	9	3088	47.65 ^a
Deviation from surface	1295	20	64.7	$F(0.05, 9, 20) = 2.39$
Trend surface, order $p + 1$	26702	5	5340	53.70 ^b
Deviation from surface	2386	24	99.4	$F(0.05, 5, 24) = 2.62$
Increase in order	1090	4	272.6	4.20 ^c
Total variance	29088	29		$F(0.05, 4, 20) = 2.87$

The number of observations is n (cf. Table 2).

^a Significance test of trend surface with order $p + 2$.

^b Significance test of trend surface with order $p + 1$.

^c Significance test of the increase in order.

ment that a first order trend surface should be sufficient to describe the relationship of EC_{sw} to depth and time. The trend surfaces representing first, second and third order polynomials were mapped for all six treatments in Fig. 3 (the surfaces are salinity contours, the shading intensity of which is proportional to the salinity degree). Fig. 3 indicates that the salinisation tendency as summer progresses from October to March was strongest at depth in the low salinity treatments but was more uniformly distributed through the soil profile in

response to more saline treatments. Since only five depth intervals were sampled, fitting a polynomial higher than the first order for a single sampling event would probably correspond to over-interpretation. In Fig. 3, treatments 1.5 and 3.5 dS m^{-1} showed differences in the general trends compared with the other treatments. These differences were associated with lower infiltration rates, as part of these treatments were affected by ancient termite nests, causing different soil water behavioural patterns. Regardless of the

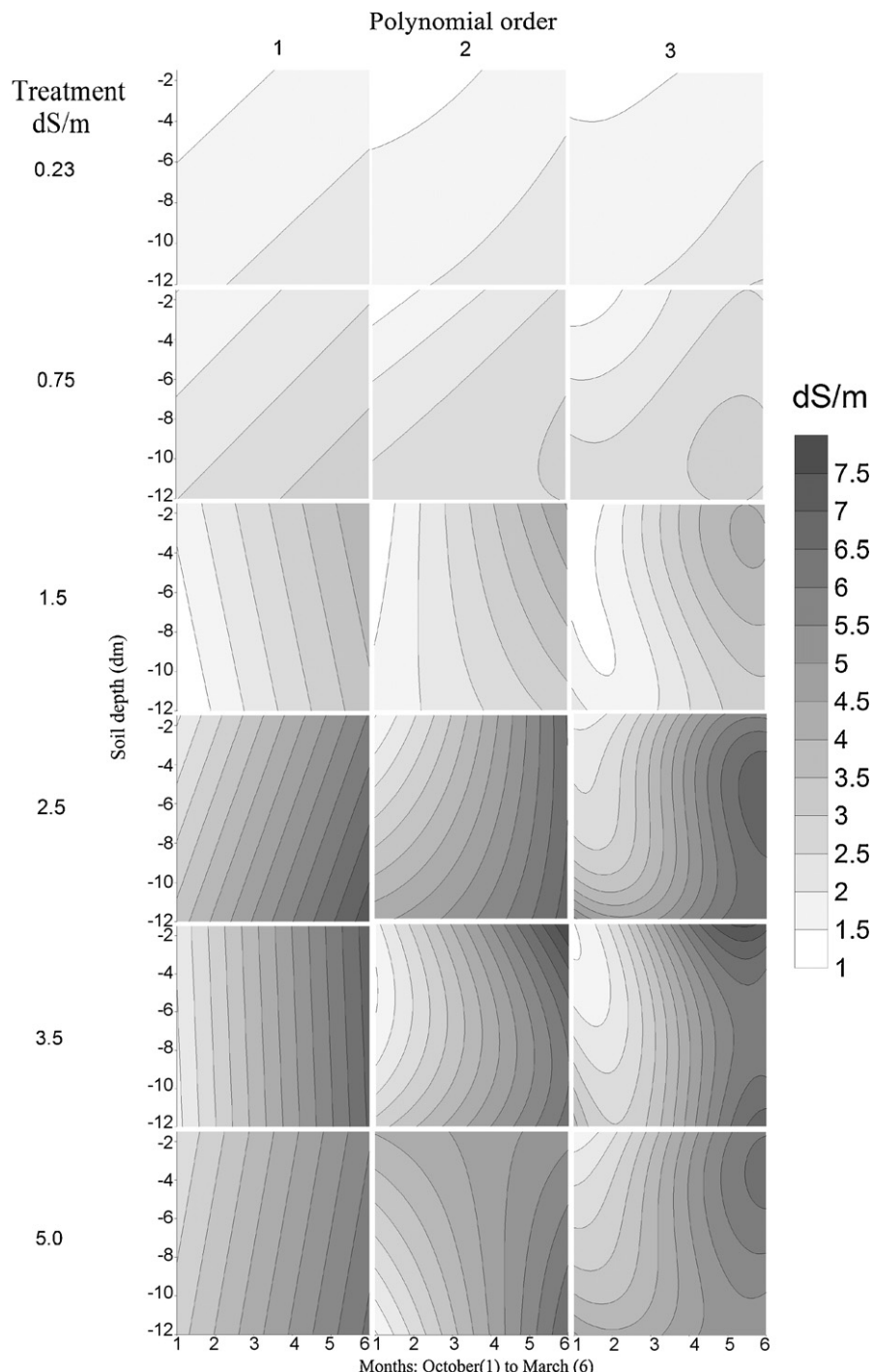


Fig. 3 – Trend surfaces represented by contours of soil water salinity (EC_{sw}) in relation to time in early summer and depth of soil in plots treated with six levels of irrigated salinity ($T_1 - T_6$; cf. Fig. 1) over 8 years. Graph columns from left to right are based on the first, 2nd and 3rd order polynomials as applied to the time to depth EC_{sw} relationships.

Table 7 – R^2 and the adjusted R^{2*} for the three trend orders

Order	R^2	R^{2*}	$R^2 - R^{2*}$
p first	0.905	0.898	0.007
p + 1 second	0.918	0.901	0.017
p + 2 third	0.955	0.935	0.020

latter, the way in which trend surface analysis was applied, combined the parameters of space and time in the test. Therefore the different sampling points in the landscape showed similar behaviour.

Table 7 shows the changes in both R^2 and R^{2*} with increasing polynomial order as was applied to the p, p + 1 and p + 2. It is clear that the difference in R^2 values has shrunk considerably by using the adjusted R^2 to such an extent that there is almost no difference between p and p + 1.

Due to the significance displayed in the first order polynomial above (Table 4), it should be possible to describe salinisation of the soil profile during an irrigation season on the basis of only two measurement depths (preferably conveniently shallow). This could enable quick estimation whether over- or under-irrigation has occurred and whether salt accumulation has taken place below the root zone. This can be indicated by knowing the gradient (m) of the first order polynomial. To determine which two monitoring depths are most suitable, the data were subjected to an analysis in which depth trend lines for each time interval were calculated from EC_{sw} measurements at two pairs of shallower depths (either 15 and 60 or 30 and 60 cm). The gradients of these EC depth trend lines were then compared with the gradients of EC lines derived from EC measurements at all five depths in Table 8. Therefore, the regression between the gradients derived from situation 1 (Table 8) and gradients derived from the 5 depth trend lines, produced a R^2 of 0.51 and a highly significant $p_{0.005}$ value of 0.0034. But, regressing the general soil EC_{sw}-profile from situation 2 (Table 8), with the 5 depth trend line gradients, produced a better R^2 value of 0.89 and a $p_{0.005}$ value of 0.0001. This shows that in about 9 out of 10 cases tested, an increase or decrease of EC_{sw} at a soil depth of 120 cm could be predicted with confidence by looking at EC_{sw} data from only two depth increments in the upper soil. The reason that the 0–15 cm depth showed a poorer result could possibly be related to the fact that ameliorants were added shortly before sampling or salt accumulated on the soil surface as an evaporite. The third depth increment, namely the 30–60 cm depth, proved to be the region where the bulk of the roots were situated and therefore where most soil water was taken up by the plant (De Clercq et al., 2001). It is clear that the predictive accuracy increases when the soil surface layer is avoided but the data for depth increment combination, situation 3 in

Table 9 – A regression analysis between predicted EC_{sw} values for the 120 cm depth (based on the 15–30 and 30–60 cm increments) and the measured 120 cm depth EC_{sw} values

R^2	S.E.	d.f.	$P_{0.005}$	F
73.9	97.4	71	0.00004	198.4

Table 8, show that inclusion of the A-horizon in the prediction still produced a useful result. This demonstrates that the use of an instrument such as the EM38 electromagnetic induction sensor could be of great value in predicting salinity depth trends in irrigated agriculture.

A further step was to test the extent to which the EC_{sw} below the root zone could be predicted using information based on measurements at the centre of the root zone. The resulting prediction is shown in Table 9, where the EC_{sw} at 120 cm depth was predicted using the EC_{sw} values at the 15–30 and 30–60 cm depth. The result as indicated in Table 9 is highly significant in predicting the quality of the water that would drain from this field. Water that drained past the bottom of the root zone is generally considered lost to drainage unless prolonged periods of under-irrigation occur in which case upward water movement and salt build-up could occur.

The modelled change in salinity depth trend through the year is illustrated in Fig. 4. To amplify the seasonal response, Fig. 5 was added to indicate the change in slope of the depth trend lines when the offset in each equation is ignored and $x = 1$. This signifies the relationships between treatments in terms of their profile inclination for the time of year. In both Figs. 4 and 5, a positive slope means low salt in the upper and high salt in the lower horizon. A negative slope indicates higher salt in the upper section of the profile. The indicated trend lines ties together at point (15;1) and is again an indication of the excellent predictive quality of the first order polynomial in these data.

The migration of the regression lines (Figs. 4 and 5), resulting from irrigation with saline water, might have been overlooked without the stating of simplified first order polynomial modelling. Knowing how the soil responds to irrigation over time has important implications for soil salinity surveys when carried out with electromagnetic induction sensors or when large areas have to be sampled for EC mapping and the prediction of return flow. Apart from using electromagnetic induction sensors, by knowing the date, irrigation water quality and being able to remotely measure the topsoil EC, estimation of both the subsoil salinity conditions and the return-flow components from such irrigated land becomes possible.

Electromagnetic sensors like the EM38 have the ability to measure at two depth intervals, usually in the order of 0–30

Table 8 – A regression between the gradient values of the 1st order polynomials derived from EC_{sw} at selected depth increments and from slope values derived from EC_{sw} at all 5 depth increments for situations 1–3

Situation	EC _{sw} at depths (cm)	Regression equation (Y = EC _{sw} , X = depth)	R^2	$P_{0.005}$
1	0–15, 30–60	Y = 0.435X + 0.469	0.51	0.0034
2	15–30, 30–60	Y = 0.482X + 0.546	0.89	0.0001
3	0–30, 30–60	Y = 0.402X + 0.526	0.65	0.0001

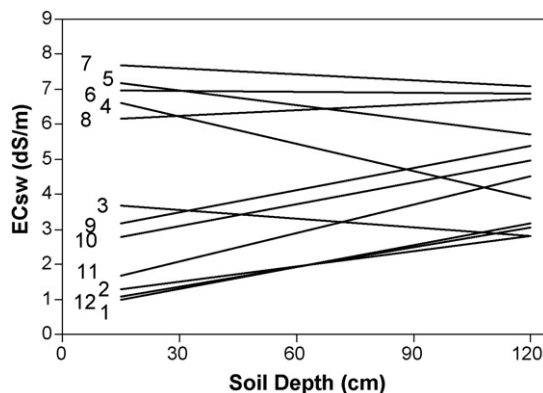


Fig. 4 – Migration of the regression lines for EC as a function of depth resulting from irrigation treatment 5 (3.5 dS m^{-1}), revealing the dynamics of EC_{sw} over time. Numbers 1–12 represent months from October to September of the following year.

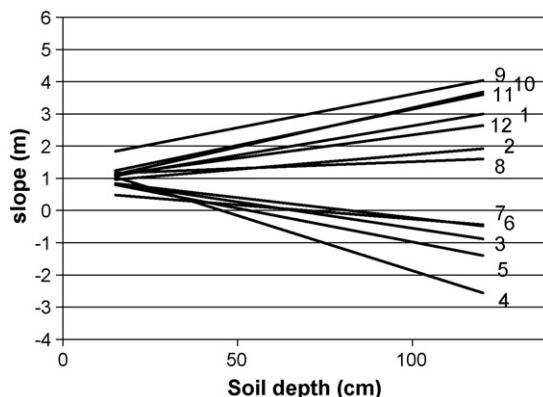


Fig. 5 – A migration of the regression lines for EC as a function of depth resulting from irrigation treatment 5 (3.5 dS m^{-1}), revealing the dynamics of slopes (m) in EC_{sw} trend lines over time ($x = 1$, offset = 0). Numbers 1–12 represent months from October to September of the following year.

and 15–120 cm. Though no EM38 data were available we feel that this approach could add considerable value to remotely sensed information. Being able to outline and link salinity depth profiles with such surveys would clearly also enhance our current remote sensing abilities. Combining information about the time of year, the remotely detected soil surface EC and the irrigation water quality, could therefore help in predicting soil profile salinity for irrigated lands.

4. Conclusions

Soil scientists often focus on unnecessary detail regarding soils and their behaviour. This study provided an opportunity to better understand the temporal and spatial variation of EC_{sw} by using a simplified approach. The classical trend

surface analysis procedure of Davis provided an answer to the problem of finding a suitable depth relationship that could be used as a norm for the soil studied. This simplified the management of salt in the soil and the quantity and quality of return flow.

Prediction of the depth trend in EC_{sw} with a first order polynomial has distinct advantages. Over- or under-irrigation can easily be evaluated for any irrigated land. Prediction of salt accumulation on the soil surface or deep drainage can readily be assessed. The slope of the first order polynomial indicates directly the general trend and whether an accumulation or a depletion of salt can be expected in the soil. When linked to remote sensing, the approach described here could be used in evaluating extensive areas of land in terms of salinity and their suitability for irrigated crops.

Lastly, this research further showed that by knowing the date, irrigation water quality and being able to characterize the topsoil EC remotely, one can estimate subsoil salinity conditions in irrigated lands and further estimate the return-flow component from such irrigated lands.

REFERENCES

- Ben-Gal, A., Ityel, E., Dudley, L., Cohen, C., Yermiyahu, U., Presnov, E., Zigmond, L., Shani, U., 2008. Effect of irrigation water salinity on transpiration and on leaching requirements: a case study for bell peppers. Agricultural Water Management 95, 587–597.
- Cetin, M., Kirda, C., 2003. Spatial and temporal changes of soil salinity in a cotton field irrigated with low-quality water. Journal of Hydrology 272, 238–249.
- Davis, J.C., 1986. Statistics and Data Analysis in Geology. Wiley, New York.
- De Clercq, W.P., Fey, M.V., Moolman, J.H., Wessels, W.P.J., Eigenhuis B., 2001. Establishing the effects of saline irrigation water and managerial options on soil properties and plant performance. WRC of South Africa Report 695/1/01.
- De Clercq, W.P., Van Meirvenne, M., 2005. Effect of long term irrigation application on the variation of soil electrical conductivity in vineyards. Geoderma 128, 221–233.
- Douaiq, A., Van Meirvenne, M., Toth, T., 2006. Temporal stability of spatial patterns of soil salinity determined from laboratory and field electrical conductivity. Arid Land Research and Management 20, 1–13.
- Farifteh, J., Farshad, A. 2002. Remote sensing and modelling of topsoil properties, a clue for assessing land degradation. 17th WCSS, Thailand, Paper 562.
- Görgens, A., De Clercq, W.P. (Eds.), 2006. Water quality information systems for integrated water resource management: The Rivieronderend-Berg River system. WRC of South Africa, Report TT262/06.
- Kelleners, T.J., Chaudhry, M.R., 1998. Drainage water salinity of tube wells and pipe drains: a case study from Pakistan. Agricultural Water Management 37, 41–53.
- Kotb, T.H.S., Watanabe, T., Ogino, Y., Tanji, K.K., 2000. Soil salinization in the Nile Delta and related policy issues in Egypt. Agricultural Water Management 43, 239–261.
- Lesch, S.M., Strauss, D.J., Rhoades, J.D., 1995. Spatial prediction of soil salinity using electromagnetic induction techniques. 2. An efficient spatial sampling algorithm suitable for multiple linear regression model identification and estimation. Water Resources Research 31, 387–398.

- Metternicht, G.I., Zinck, J.A., 2003. Remote sensing of soil salinity: potentials and constraints. *Remote Sensing of Environment* 85, 1–20.
- Mondala, M.K., Bhuiyan, S.I., Franco, D.T., 2001. Soil salinity reduction and prediction of salt dynamics in the coastal rice lands of Bangladesh. *Agricultural Water Management* 47, 9–23.
- Nelson, P.N., Ham, G.J., 2000. Exploring the response of sugar cane to sodic and saline conditions through natural variation in the field. *Field Crops Research* 66, 245–255.
- Odeh, I.O.A., Todd, A.J., Triantifilis, J., McBratney, A.B., 1998. Status and trends of soil salinity at different scales: the case for the irrigated cotton growing region of eastern Australia. *Nutrient Cycling in Agroecosystems* 50, 99–107.
- Persson, M., Bertacchi Uvo, C., 2003. Estimating soil solution electrical conductivity from time domain reflectometry measurements using neural networks. *Journal of Hydrology* 273, 249–256.
- Rhoades, J.D., Lesch, S.M., LeMert, R.D., Alves, W.J., 1997. Assessing irrigation/drainage/salinity management using spatially referenced salinity measurements. *Agricultural Water Management* 35, 147–165.
- Saayman, D., 1988. The role of environment and cultural aspects in the production of table, raisin and wine grapes in South Africa. *I. Deciduous Fruit Grower* 38, 60–65.
- Shani, U., Ben-Gal, A., Tripler, E., Dudley, L.M., 2007. Plant response to the soil environment: an analytical model integrating yield, water, soil type and salinity. *Water Resource Research* 43 W08418 10.1029/2006WR005313.
- Sharma, D.P., Rao, K.V.G.K., 1998. Strategy for long term use of saline drainage water for irrigation in semi-arid regions. *Soil & Tillage Research* 48, 287–295.
- Shi Zhou, Jie-Liang, C., Ming-Xiang, H., Lian-Qing, Z., 2006. Assessing reclamation levels of coastal saline lands with integrated stepwise discriminant analysis and laboratory hyperspectral data. *Pedosphere* 16, 154–160.
- Soil classification working group, 1991. Soil classification: a taxonomic system for South Africa. ISCW, Pretoria.
- Van Zyl, J.L., 1984. Response of colombar grapevines to irrigation as regards quality aspects and growth. *South African Journal of Enology and Viticulture* 5, 19–28.
- Zhu, Y., Cao, W.X., Dai, T.B., Tian, Y.C., Yao, X., 2007. A knowledge model system for wheat production management. *Pedosphere* 17, 172–181.